

Alternative seismic hoop details for reinforced concrete columns in low rise buildings

*Chul-Goo Kim¹⁾, Hong-Gun Park²⁾, Tae-Sung Eom³⁾, and Tae-Wan Kim⁴⁾

^{1), 2)} *Department of Architecture, Seoul National University, Seoul 151-744, Korea*

³⁾ *Department of Architectural engineering, Dankook University, Yongin 448-701, Korea*

⁴⁾ *Division of Urban, Design & Architecture, Kangwon National University, Chuncheon 200-701, Korea*

¹⁾ these09@naver.com

²⁾ parkhg@snu.ac.kr

³⁾ tseom@dankook.ac.kr

⁴⁾ tkim@kangwon.ac.kr

ABSTRACT

In one or two story small buildings, since the cross-section of the columns is smaller than that of the beams, plastic hinge zones develop in the columns rather than beams. In the present study, the effect of various tie details on the seismic performance of such columns was studied. Three square columns and four rectangular columns were tested under lateral cyclic loading. The primary test parameters were the cross-section shape and tie details. Considering constructability in small buildings, various tie details including non-seismic details were considered. For example, in consecutive ties, the locations of the 90 degree hook anchorages were alternated to restrain unfolding of the hooks under cyclic loading. The test results showed that columns with such lap spliced ties, U-shaped ties, and 90 degree hook ties showed good seismic performances under cyclic loading, though the deformation capacities were slightly less than those of the columns with conventional seismic details.

1. INTRODUCTION

Generally, one or two story small buildings show weak column-strong beam behavior under seismic loads as the size of columns is smaller than that of the beams. Thus, to assure the safety of the structures, the ductility of the columns should be enhanced. In high seismic zones, seismic details including hoop details (135 degree hooks) and spacing ($s \leq 0.25H_{\min}$) are required for the ties of columns (ACI 318). On the other hand, in moderate seismic zone, such strict details may not be required, and it is expected that alternative details can be used for better constructability, satisfying the minimum requirement of ductility.

¹⁾ Graduate Student

²⁾ Professor

³⁾ Professor

⁴⁾ Professor

Thus, in the present study, alternative seismic details for column ties were studied. As a result, alternative hoops using 90 degree hooks, U shaped ties, and lap splice hoops were selected, considering constructability and economy. For verification, columns using the alternative hoops were tested under cyclic lateral loading and low compression force. On the basis of the test results, the effects of various hoop details on the seismic performance of reinforced concrete columns were evaluated.

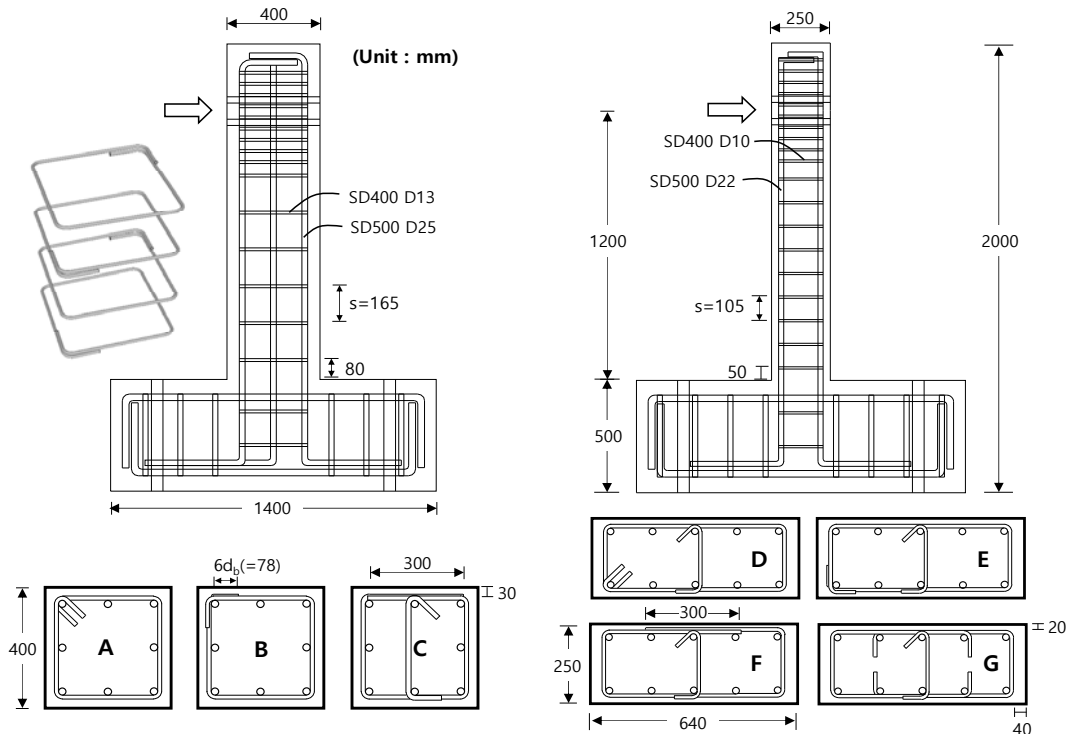
2. TEST PROGRAM

Cyclic loading tests for cantilever columns were conducted to evaluate the performance of various hoop details. The level of the axial loads was $0.1 \sim 0.2 A_g f_{ck}$ (A_g : corss sectional area; f_{ck} : concrete compressive strength).

2.1 Test parameters

Seven column specimens were tested. The configurations of the columns and the hoop details are shown in Fig. 1. The dimensions of the cross-sections were 400 mm x 400 mm for square columns and 250mm x 640 mm for rectangular columns.

Four hoop details were studied: 135 degree hooks(A, D), 90 degree hooks(B, E), lap splice(C, F), and U shape hoops(G). Although the 135 degree hooks show superior performances, the alternative hoop details can provide better constructability, satisfying the minimum ductility requirement of small buildings in moderate seismic zones. In the lap spliced hoops, the lap splice length was 300 mm. In the U shaped hoops, 90 degree hook anchorages were used at the ends.



(a) Square column (b) Rectangular column
Fig. 1 Details of hoops and specimens

2.2 Test specimens

Square specimens SAd2 to SCd2 have 135 degree hooks, 90 degree hooks, and lap splice hoops, respectively. Rectangular specimens RDd2 to RGd2 have 135 degree hooks, 90 degree hooks, lap splice hoops, and U shape hoops, respectively. Fig. 1 shows reinforcement details of square and rectangular columns. Grade 500MPa and 400MPa bars were used for longitudinal and transverse reinforcing bars, respectively. The square columns had D25 (Deformed bars, diameter=25mm) and D13 bars and the rectangular columns had D22 and D10 reinforcing bars for the longitudinal and transverse reinforcing bars, respectively.

The hoop spacing was assumed to be half of the effective depth of the columns ($s=0.5d$), considering the spacing requirement of shear reinforcement: 165mm for square columns and 105 mm for rectangular columns. The first hoops were started from 80mm and 50mm above the base in square and rectangular columns, respectively. In the case of hoops using 90 degree hooks, to restrain unfolding of the anchorage, the location of the hooks was alternated (i.e. 180 degree rotation) every hoop as shown in Fig. 1.

2.3 Test setup and loading protocol

Fig. 2 shows the test setup. An oil pump was used to apply axial load, and an actuator was used for lateral loading. For test measurements, load cells, LVDTs, and strain gauges were used.

The loading protocol in Fig. 3 was planned according to ACI374.1. The first lateral drift ratio (Δ/L) was 0.25% in the elastic range. Then, the drift ratio was increased in the rate of 1.25 ~ 1.5 times the previous drift. The cyclic loading was repeated three times in a drift level and was terminated when the post-peak load decreased to 80% of the peak load. In the case of rectangular sections, the lateral load was applied in the direction of the short side of the cross-section.

2.4 Material properties

Six concrete cylinders were tested on the day of column tests. The average compression strength of concrete cylinders was 32 MPa. The maximum aggregate size was 25 mm.

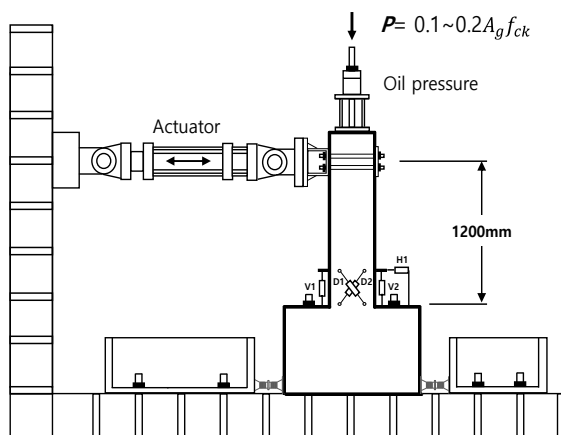


Fig. 2 Test setup

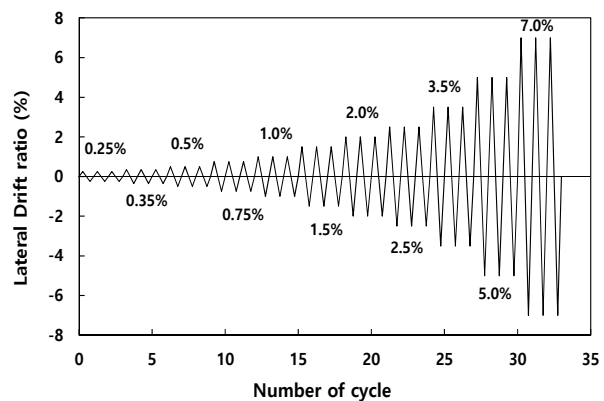


Fig. 3 Loading protocol

The yield strengths (f_y) of the re-bars were 530 MPa for D10 bars, 500 MPa for D13 bars, 566 MPa for D22 bars, 571 MPa for D25 bars.

3. TEST RESULTS

3.1 Lateral load – drift ratio relationships

The test results (hysteretic and envelope curves) of the square columns are shown in Fig. 4. The peak loads (V_u) and predicted loads (V_n), which were calculated by sectional analysis, are compared in Fig. 4(a) ~ (c). The maximum loads were 315 ~ 339 kN in the positive direction and -331 ~ -343 kN in the negative direction. The ratios of the test strength to the prediction were 1.01 ~ 1.10, which indicates that the hoop details did not affect the maximum strength.

The maximum lateral drift ratio, in this study, was defined as the post-peak drift ratio of the third loading cycle corresponding to the 80 percent of the peak load. The 135 degree hook specimen (SAd2) showed the greatest lateral drift ratio, 3.5%, while the 90 degree hook specimen (SBd2) and the lap splice specimen (SCd2) showed 2.5%.

Fig. 4(d) shows the envelope curves of the square columns. The envelope curve was defined by connecting the peak point of the first load cycle at each drift ratio. The test specimens show similar behaviors in terms of stiffness and maximum load.

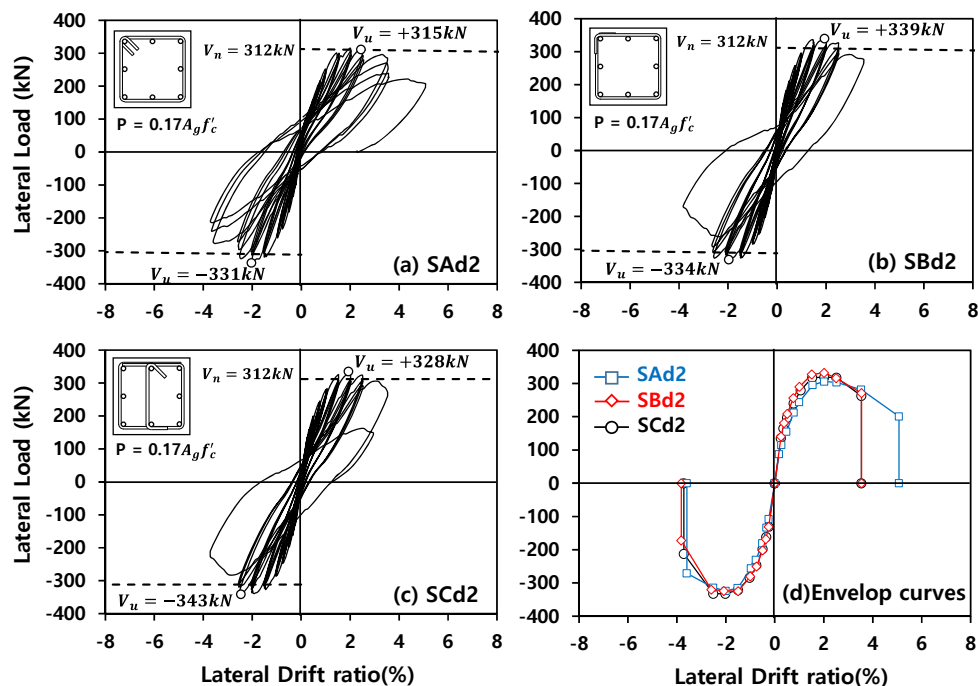


Fig. 4 Lateral load – drift ratio relationships of square columns

The test results of the rectangular columns are shown in Fig. 5. The peak loads (V_u) and predicted loads (V_n) are also compared in Fig. 5(a) ~ (d). The maximum loads were 203 ~ 240 kN in the positive direction and -213 ~ -251 kN in the negative direction. The ratios of the test strength to the prediction were 1.01 ~ 1.15, which indicates that the hoop details did not affect the maximum strength.

The cyclic tests were terminated at the 7.0% drift ratio due to the limited stroke length of the actuator. The 135 degree hook specimen (RDd2) and U type bar specimen (RGd2) showed the greatest lateral drift ratio, 7.0%, while the 90 degree hook specimen (REd2) and the lap splice specimen (RFd2) showed 3.5% and 5.0%, respectively.

Fig. 5(e) shows the envelope curves of the rectangular columns. The test specimens showed different behaviors in terms of stiffness and lateral drift. Specimen RDd2, which was subjected to relatively low compressive force, $0.1A_gf_c$, showed smaller peak load and stiffness than the other specimens. Specimen REd2 with 90 degree hooks showed smaller lateral drift ratio than the other specimens using alternative hoops.

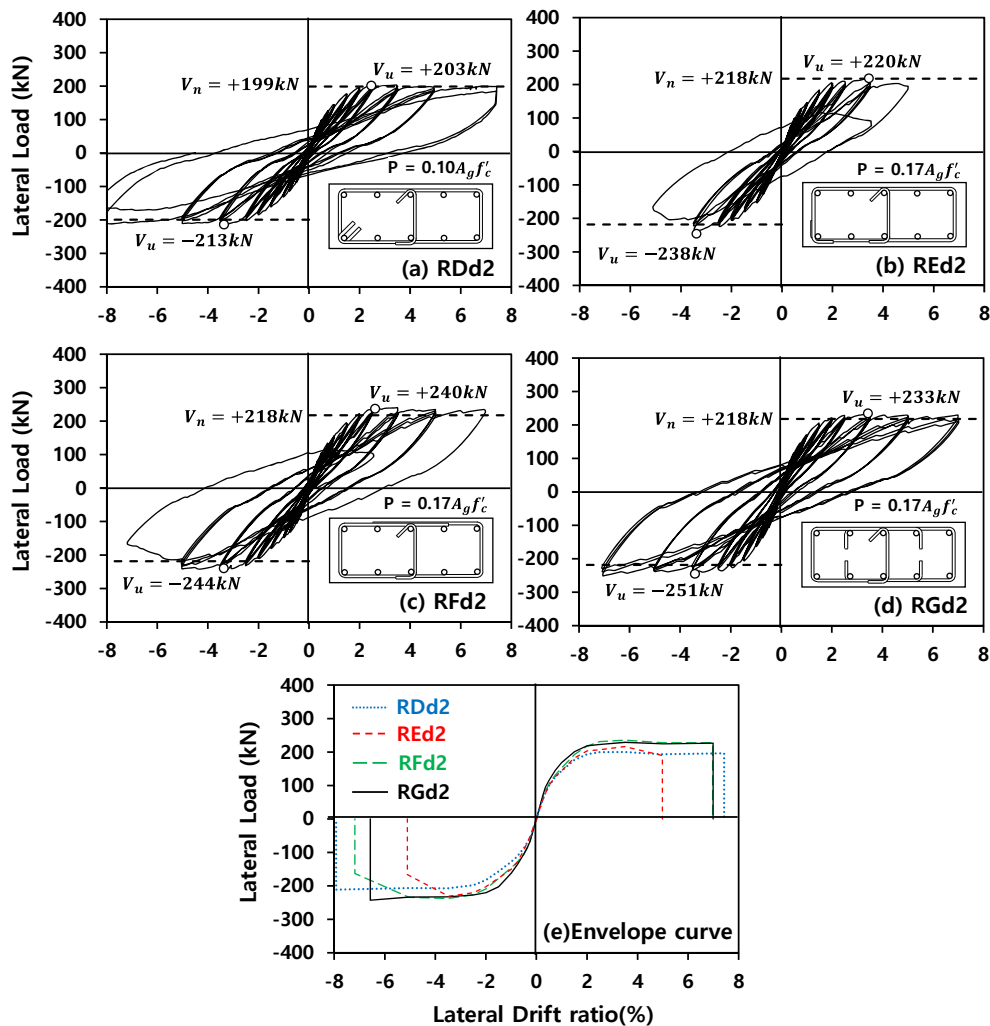


Fig. 5 Lateral load – drift ratio relationships of rectangular columns

3.2 Failure mode

Fig. 6 shows damage propagations of specimens SAd2 and RDd2. The damage propagation of SAd2 was as follows: 1) flexural cracking at the 0.75% drift ratio, 2) diagonal cracking in the plastic hinge zone at 1.5%, 3) concrete cover spalling at 2.0%, and 4) confinement failure of the core concrete at 5.0%. On the other hand, the damage propagation of RDd2 was as follows: 1) flexural cracking at 2.0%, 2) concrete cover spalling at 3.5%, 3) diagonal cracking at 5.0%, and 4) flexural failure at 7.0%. The square columns showed flexure-shear failure, whereas the rectangular columns showed flexural failure. This is because the shear span ratio of the square columns, $a/H=3.0$, was smaller than that of the rectangular columns, $a/H=4.8$.

Fig. 7 shows the crack patterns of the test specimens at the end of tests. In the square columns, large flexural and diagonal shear cracks occurred in the plastic hinge zone. Diagonal cracks propagated to the loading points. The 90 degree hook (SBd2) and lap spliced hoop (SCd2) were loosened and unfolded. On the other hand, the rectangular columns had relatively a small amount of diagonal cracks, but concrete at the plastic hinge zone was severely damaged by flexural moment. The 135 degree hook (RDd2) was fractured by buckling of the longitudinal bars though the hoops were not unfolded. The 90 degree hook (REd2) and lap spliced hoop (RFd2) also failed due to buckling of the longitudinal bars. The U type bar with 90 degree hooks (RGd2) did not fail until 7.0% lateral drift ratio.

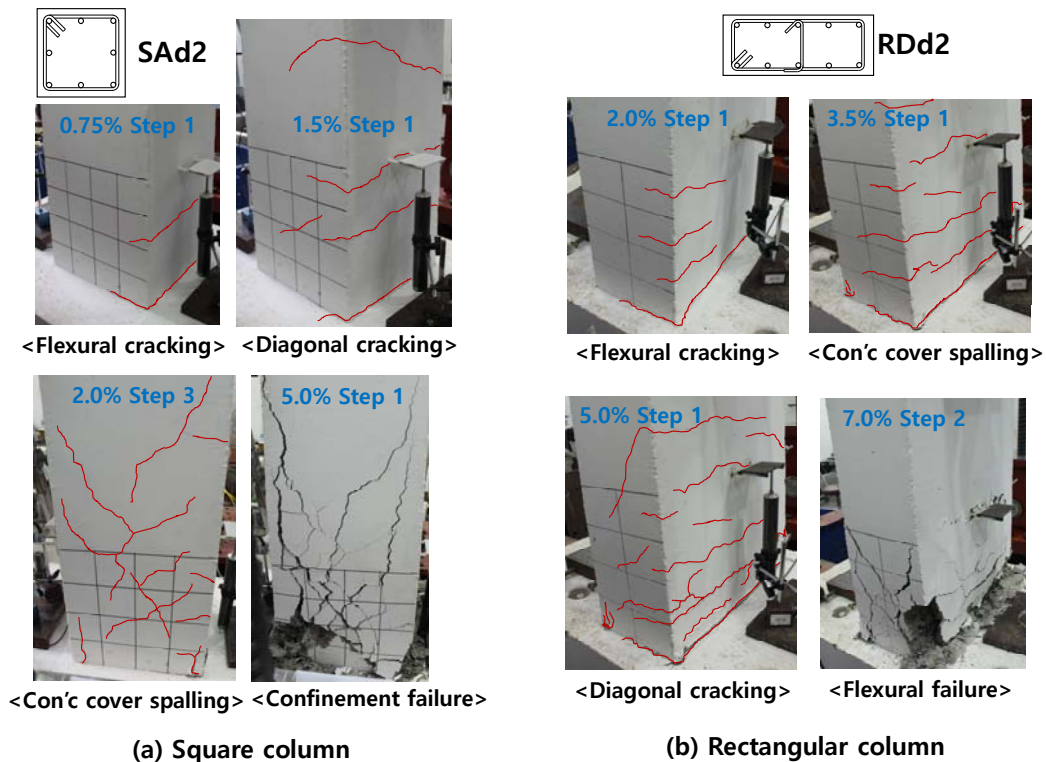


Fig. 6 Failure modes of test specimens according to drift ratio

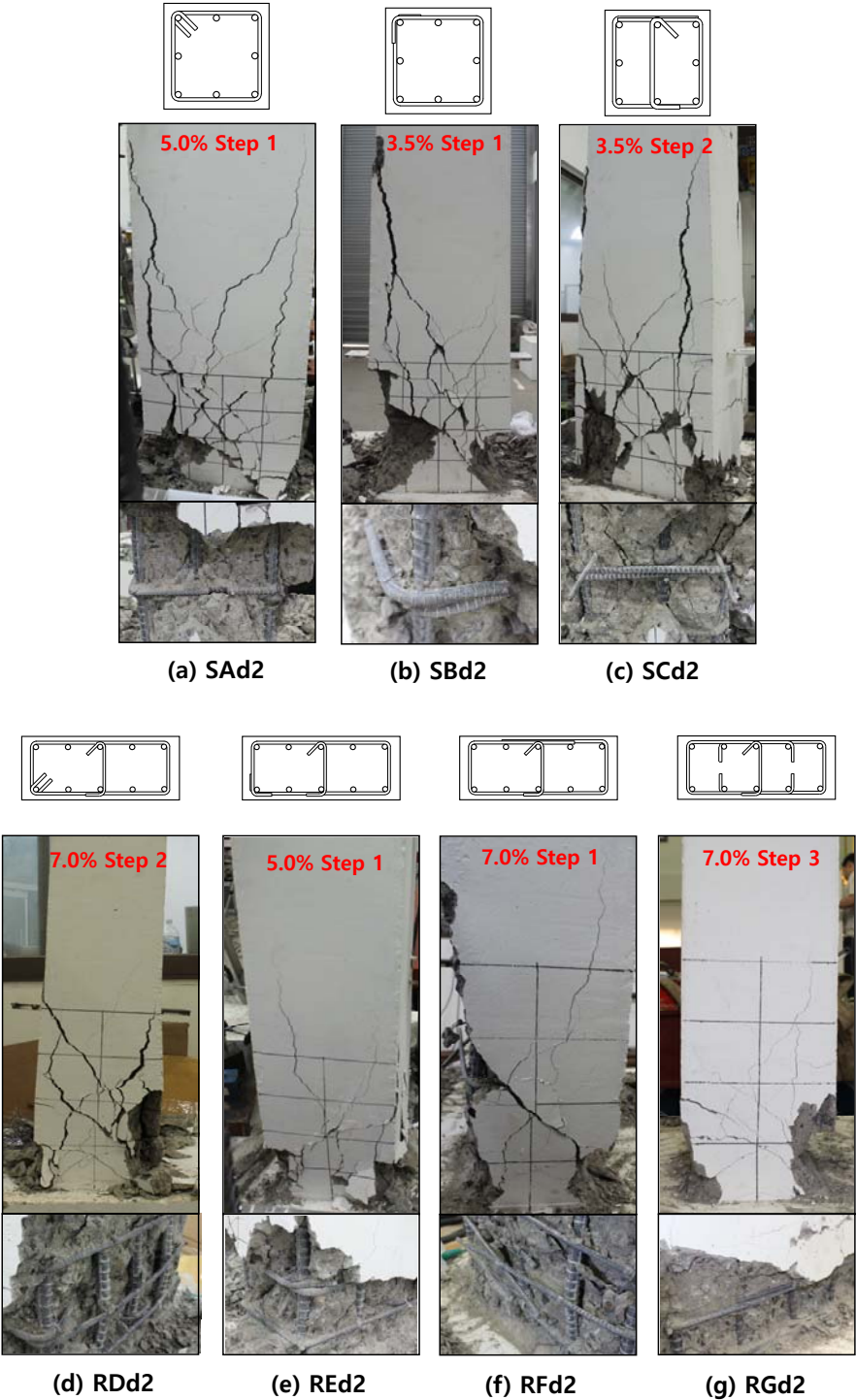
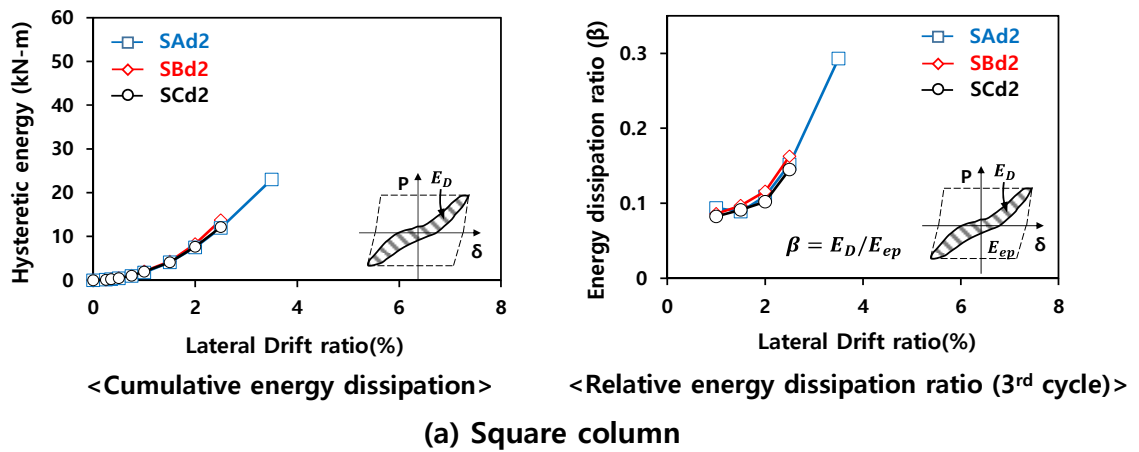


Fig. 7 Crack patterns of test specimens at the end of test

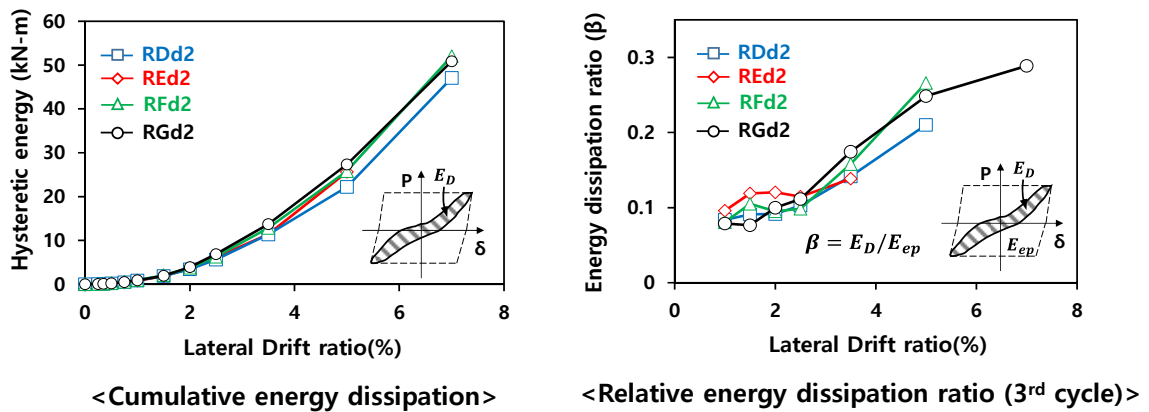
3.3 Energy dissipation

Fig. 8 shows the cumulative energy dissipation and relative energy dissipation ratio of the test specimens. The cumulative energy dissipation is the total energy absorption during cyclic loadings. The relative energy dissipation ratio (β) is defined as the ratio of the actual energy dissipation (E_D) to the idealized energy dissipation (E_{ep}) corresponding to the elasto-perfectly plastic behavior.

In Fig. 8, the energy dissipations of the square columns were the same until 2.5% drift ratio. Also in the case of the rectangular columns, the energy dissipation were close except for specimen RDd2 under relatively low compressive force ($0.1A_g f_c'$). The rectangular columns dissipated more energy than the square columns because the rectangular columns showed greater inelastic deformations.



(a) Square column



(b) Rectangular column

Fig. 8 Cumulative energy dissipation and relative energy dissipation ratio

4. ANALYSIS OF TEST RESULTS

4.1 Effective stiffness

The effective stiffness (K_e) was estimated based on test results of load versus lateral drift relationships. In the previous studies, the effective stiffness was defined by secant stiffness on 75% of maximum load proposed by Park (1988), on 70% of maximum load by Elwood and Moehle(2005), on 80% of maximum load by Elwood and Eberhard(2009). In this study, the method of Park (1988) was used as shown in Fig. 9.

Table 1 presents the effective stiffness (K_e and K_{eff}) based on test results and ASCE 41-13. ASCE41 presents the effective stiffness as follows.

$$K_{eff} = \begin{cases} 0.3E_c I_g \left(\frac{3}{a^3} \right) & \text{for } \frac{P}{A_g f'_c} < 0.1 \\ \left(\frac{P}{A_g f'_c} + 0.2 \right) E_c I_g \left(\frac{3}{a^3} \right) & \text{for } 0.1 \leq \frac{P}{A_g f'_c} < 0.5 \\ 0.7E_c I_g \left(\frac{3}{a^3} \right) & \text{for } \frac{P}{A_g f'_c} \geq 0.5 \end{cases} \quad (1)$$

The ratio (K_e/K_{eff}) is 0.58~0.78 in the case of square columns and 0.69~0.97 in the case of rectangular columns. Overall, K_{eff} from ASCE41 is much higher than K_e from test results. The effective stiffness of the alternative details might be estimated to be less than that from ASCE41.

Table 1 Effective stiffness of test results and ASCE41

Specimen	Positive direction			Negative direction		
	K_e (kN/mm)	K_{eff} (kN/mm)	K_e/K_{eff}	K_e (kN/mm)	K_{eff} (kN/mm)	K_e/K_{eff}
SAd2	21.4	37	0.58	23.2	37	0.63
SBd2	29.0	37	0.78	28.6	37	0.77
SCd2	26.4	37	0.71	26.7	37	0.72
RDd2	11.4	11.7	0.97	8.7	11.7	0.74
REd2	11	14.4	0.76	10.1	14.4	0.70
RFd2	11.3	14.4	0.78	9.9	14.4	0.69
RGd2	13.7	14.4	0.95	12.1	14.4	0.84

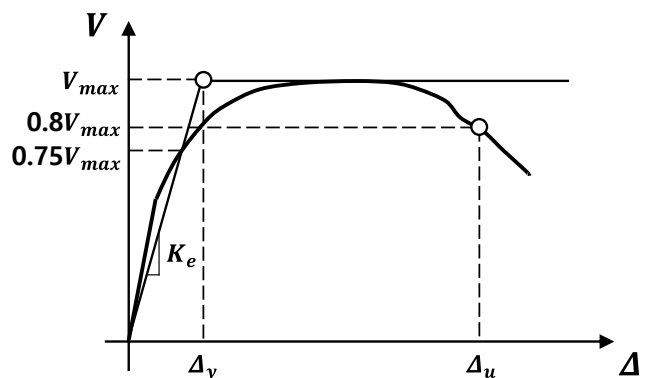


Fig. 9 Effective stiffness based on test results

4.2 Force-deformation envelop curves

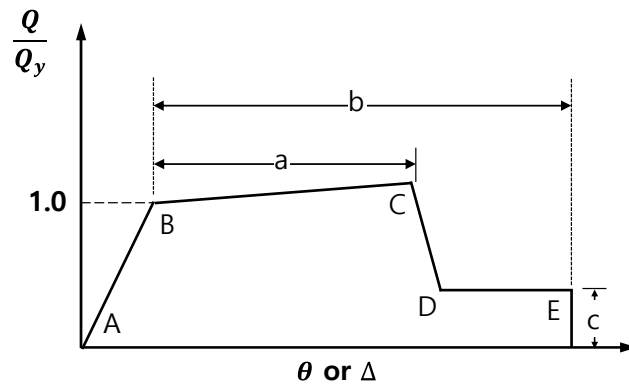
Force-deformation relationships as shown in Fig. 10 should be defined for nonlinear analysis. ASCE41 presents generalized force-deformation relations of each member through nonlinear modeling parameters. The procedure for estimating nonlinear modeling parameters is as follows.

Failure modes i ~ iii (Flexural, flexural-shear, shear) are classified based on the shear capacity ratio (V_p/V_o) and transverse reinforcement details. On the basis of the failure modes, nonlinear modeling parameters (a ~ c in Table 2) are determined according to expected axial load, shear reinforcement ratio, and design shear force.

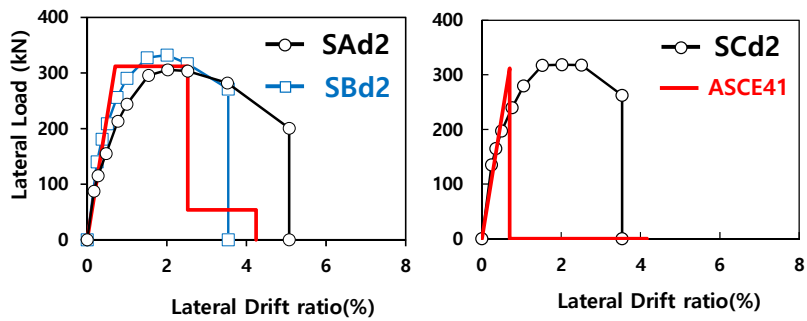
Fig. 10 shows comparison between envelope curves of test results and force-deformation relations predicted by ASCE41. The initial stiffness of predicted curves is from the value K_{eff} in Table 1. The nonlinear modeling parameters and properties of each specimen are presented in Table 2. The 135 degree hooks (SAd2, RDd2) and 90 degree hooks specimens (SBd2, REd2) have failure mode ii corresponding to flexural shear failure. Whereas, lap spliced and U type hoop specimens (SCd2, RFd2, RGd2) have failure mode iii corresponding to shear failure. For the specimens SCd2, RFd2, and RGd2, the modeling parameters 'a' and 'c' are zero from Table 10-8 of ASCE41. Thus, the plastic behaviors of these specimens cannot be considered by predictions of ASCE41, even though the test results show the additional deformations after the flexural yielding.

Table 2 Nonlinear modeling parameters of test specimens

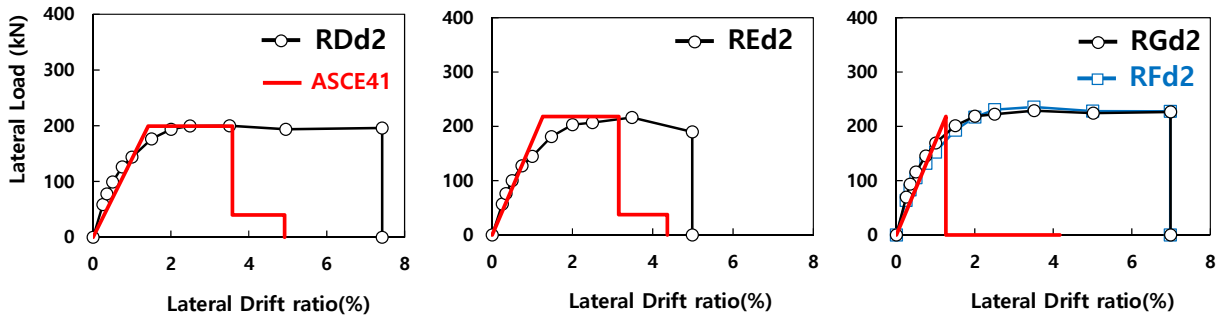
Specimen	V_o (kN)	V_p (kN)	$\frac{V_p}{V_o}$	Tie detail	Conditions	s (mm)	ρ_{trans} (%)	Axial load	$\frac{V}{b_w d \sqrt{f'_c}}$	Modeling parameter		
										a	b	c
SAd2	449	312	0.69	135°	ii	165	0.39	$0.17 A_g f'_c$	0.41	0.0182	0.0354	0.172
SBd2	449	312	0.69	90°	ii	165	0.39	$0.17 A_g f'_c$	0.41	0.0182	0.0354	0.172
SCd2	449	312	0.69	Lap splice	iii	165	0.39	$0.17 A_g f'_c$	0.41	0	0.0346	0
RDd2	317	199	0.63	135°	ii	105	0.32	$0.10 A_g f'_c$	0.26	0.0216	0.035	0.2
REd2	332	218	0.66	90°	ii	105	0.32	$0.17 A_g f'_c$	0.29	0.0189	0.031	0.172
RFd2	332	218	0.66	Lap splice	iii	105	0.32	$0.17 A_g f'_c$	0.29	0	0.029	0
RGd2	332	218	0.66	U-bar	iii	105	0.32	$0.17 A_g f'_c$	0.29	0	0.029	0



(a) Generalized force-deformation relation



(b) Square column



(c) Rectangular column

Fig. 10 Comparison of test results and ASCE41-13

5. CONCLUSIONS

In the present study, for constructability and economy, alternative seismic hoop details were proposed. Cyclic loading tests were performed to evaluate the seismic performance of square and rectangular columns with various hoop details. The effects of hoop details were compared regarding the failure modes and deformation capacities. The test results were compared with the predicted value of ASCE41-13 in terms of the initial stiffness and force-deformation relations. The major findings of this study are summarized as follows:

- 1) The square columns experienced diagonal shear failure after flexural yielding in the range of 2.5~3.5% drift ratio. On the other hand, the rectangular columns with relatively larger shear span showed ductile behavior after flexural yielding, showing 5.0~7.0% drift ratio. The hoop details did not affect the peak load. On the other hand, the use of alternative hoop details decreased the deformation capacity, when compared to the conventional seismic hoop detail.
- 2) The non-conventional alternative hoops having 90 degree hooks and lap spliced hoops were vulnerable to unfolding which is caused by buckling of longitudinal bars after crushing of the core concrete. Nevertheless, the alternative hoops maintained ductile behavior until 2.5% drift ratio (in the case of square sections).
- 3) The effective stiffness ratio of the test results to the prediction of ASCE41 was 0.58 ~ 0.78 in the square columns and 0.69 ~ 0.97 in the rectangular columns. The result indicates that the prediction of ASCE41 was closer to the test results of rectangular columns. This is because the effective stiffness of ASCE41 was proposed on the basis of flexural deformations.
- 4) The envelop curves of the test results were compared with the load-deformation relationships predicted by ASCE41. The prediction of ASCE41 was comparable to the test results. However, in the case of the alternative hoop details using lap splice and U type hoop, ASCE41 excessively underestimate the deformation capacity. This is because plastic behavior is not permitted in the ASCE 41, when such alternative details are used.
- 5) On the basis of the test results, the followings are recommended for seismic design of columns in low rise buildings in moderate seismic zone: in the case of square columns (section dimensions = 400 x 400mm), at least, 2.5 % drift ratio can be achieved by using the alternative hoops details; in the case of hoops using 90 degree hooks, to restrain unfolding of the anchorage, the location of the hooks was alternated (i.e. 180 degree rotation) every hoop as shown in Fig. 1; and the maximum hoop spacing of columns should be limited to half of the minimum width of the cross section ($0.5h_{\min}$).

ACKNOWLEDGEMENTS

This research was supported by a grant (Code 13AUDP-B066083-01) from R&D Policy Infra program funded by Ministry of Land, Infrastructure and Transportation (MOLIT) of Korean government. The authors are grateful for their supports.

REFERENCES

- ACI 318 (2011), Building code requirements for structural concrete and commentary, American Concrete Institute, Michigan.
- ACI 374.1 (2005), Acceptance criteria for moment frames based on structural testing and commentary, American Concrete Institute, Michigan.
- ASCE/SEI41 (2013), Acceptance criteria for moment frames based on structural testing and commentary, American Concrete Institute, Michigan.
- Elwood, K.J., Moehle, J.P. (2005), "Drift capacity of reinforced concrete columns with light transverse reinforcement", *Earthquake Spectra*, **21**(1), 71-89.
- Elwood, K.J., Eberhard M.O. (2009), "Effective stiffness of reinforced concrete columns", *ACI Str. J.*, **106**(4), 476-484.
- Park, R. (1988), "Ductility evaluation from laboratory and analytical testing", *Proceedings of the 9th World Conference on Earthquake Engineering*, Tokyo-Kyoto.